MULTIBODY DYNAMICS 2007, ECCOMAS Thematic Conference
C.L. Bottasso, P. Masarati, L. Trainelli (eds.)
Milano, Italy, 25–28 June 2007

AN ANALYSIS OF EQUIVALENT IMPEDANCE CHARACTERISTICS BY MODELING THE HUMAN MUSCULOSKELETAL STRUCTURE AS A MULTIBODY SYSTEM

Masatoshi Hada[⋆], Daisuke Yamada[⋆], and Toshio Tsuji[†]

[⋆] TOYOTA Central Research & Development Laboratories, Incorporated
Nagakute, Aichi, 480–1192, Japan
e-mails: hada@vdlab.tytlabs.co.jp, d-yamada@mosk.tytlabs.co.jp,
web page:http://www.tytlabs.co.jp

[†] Graduate School of Engineering, Hiroshima University
1–4–1 Kagamiyama, Higashi-Hiroshima, 739–8527, Japan
e-mail: tsuji@bsys.hiroshima-u.ac.jp,
web page:http://www.bsys.hiroshima-u.ac.jp

Keywords: Equivalent impedance, Human-machine system, Multibody dynamics, Musculoskeletal system, Muscle-tendon complex

Abstract.

This paper deals with an analysis of equivalent impedance characteristics of human-machine systems taking contact and constraint conditions into account. The analysis consists of four phases: modeling human-machine system, solving the equation of motion, deriving equivalent impedance characteristics, and visualizing the results. First, each muscle tendon complex of the human is modeled as a Hill-type model and the muscle path as a series of line segments with viapoints using a wrapping technique. Then differential-algebraic equations (DAEs) of the human-machine system are formulated by modeling both of the human musculoskeletal structure and the object as the unified multibody system. Next, the joint torque of the human and the generalized forces of the object are obtained from inverse dynamics using motion and external force data. Muscle forces are estimated using a sequential quadratic programming with maintaining a balance against the joint torque. In the analysis phase, muscle stiffness and viscosity are calculated from the Hill-type model. According to coordinate transformation of tensor, human muscle impedance is transformed into reference points defined on the object, and they are synthesized with the object impedance so that equivalent impedance of the human-machine system then be obtained. The results are visualized three-dimensionally to enhance usefulness of the analysis. An upper extremities motion in forklift steering operation was analyzed as an application example. Equivalent inertia and stiffness at the human hand and around a steering column are calculated. The results show an effectiveness of the equivalent impedance analysis to investigate driver's strategy in a steering maneuver.

1 INTRODUCTION

When driving a vehicle on a bumpy road, we sometimes grasp the steering wheel of the vehicle more strongly than on a flat road. Grasping is orthogonal to the steering torque that is a control input for traveling direction of the vehicle. It is believed that human beings subconsciously perform other task than turning the steering wheel, with applying this unnecessary-like effort. It is well known that muscles, only actuator for movements of human beings, provide various viscoelastic characteristics from environmental inputs [1]. Considering mechanical impedance characteristics of both the human musculoskeletal structures and the object he/she is manipulating together, it might be possible to clarify the physical significance of the skillful strategies of human beings.

In the researches that analyze dynamics of the human musculoskeletal system, there are several software systems have been proposed. Delp et al.[2] firstly developed a software package called SIMM that enables users to develop, alter, and evaluate three dimensional musculoskeletal structures. Eberhard el al.[3] has also investigated dynamical analysis of human motion by combining musculoskeletal structure modeling and optimal control techniques. Rasmussen et al.[4] has proposed the software system called AnyBody and Nakamura et al.[5] has reported same sort of software. The users of these system specify the surfaces of bones, the kinematics and passive torque characteristics of the joints, the muscle path and force generating parameters of the muscles. Then the softwares estimate muscle forces during movement by solving inverse dynamics and optimization, or generate human motion by integrating forward dynamics from controlled input forces. These softwares can be effective in the case of human motion analysis. However, they have not yet led to analyze equivalent impedance characteristics of human-machine systems.

Some studies have been undertaken for simulating the impedance characteristics of human musculoskeletal systems. Takeda et al.[6] expressed the viscoelastic properties of muscles by polynomial formula in a joint space using experimental data, and proposed a method to express the impedance characteristics of a human hand in a task space. Furthermore, Stroeve [7] calculated the equivalent impedance characteristics of an upper extremities taking the dynamics, from the motor-command to the muscle contraction, into consideration. However, these studies were not extended to include both the viscoelastic properties of the object and the constraint conditions. In almost all of the operations, both the human and the objects are constrained in a variety of ways. Therefore, it is difficult to directly apply these studies to a practical situation where a human operates on an object.

In this paper, we propose a method for analyzing equivalent impedance characteristics of human-machine systems taking both contact and constraint conditions into account. As shown in Fig.1, this analysis consists of four phases: modeling human-machine system, solving the equation of motion, deriving equivalent impedance characteristics, and visualizing the results. First, each muscle tendon complex of the human is modeled as a Hill-type model and the muscle path as a series of line segments with viapoints using a wrapping technique. Then differential-algebraic equations (DAEs) of the human-machine system are formulated by modeling both of the human musculoskeletal structure and the object as the unified multibody system. Next, the joint torque of the human and the generalized forces of the object are obtained from inverse dynamics using motion and external force data. Muscle forces are estimated using a sequential quadratic programming with maintaining a balance against the joint torque. In the analysis phase, muscle stiffness and viscosity are calculated from the Hill-type model. According to coordinate transformation of tensor, human muscle impedance is transformed into reference

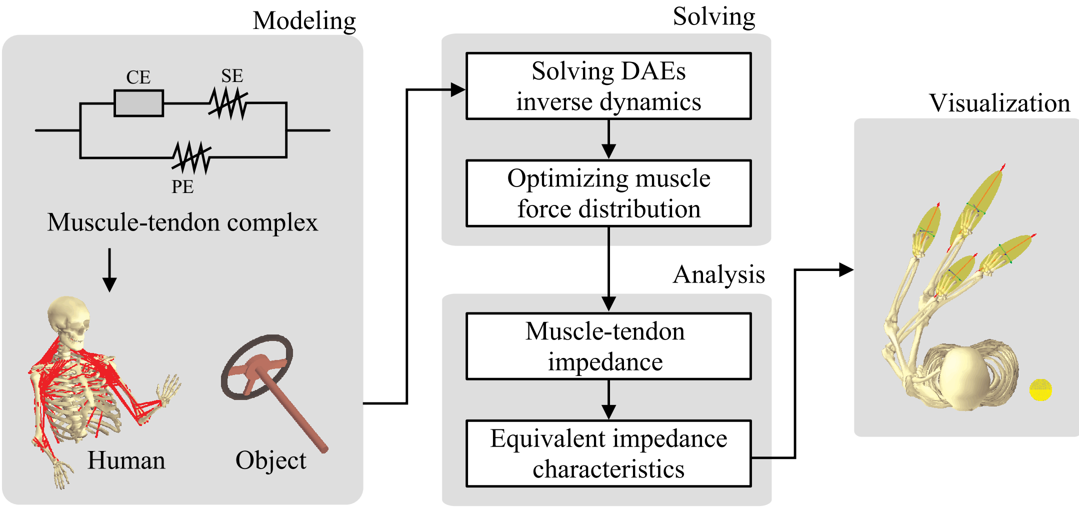

Figure 1: Overview of equivalent impedance characteristics analysis.

points defined on the object, and they are synthesized with the object impedance so that equivalent impedance of the human-machine system then be obtained. In this derivation, contact and constraint conditions are taken into account by using orthogonal complementary projections to the null space of the contacts and constraints. The results are visualized three-dimensionally to enhance usefulness of the analysis. An upper extremities motion in forklift steering operation was analyzed as an application example. Equivalent inertia and stiffness at the human hand and around steering column are calculated. The results show an effectiveness of the equivalent impedance analysis to investigate driver's strategy in a steering maneuver.

In the following discussion, muscle refers to the muscle-tendon complex unless otherwise stated. When the muscle and tendon are compared, muscle refers to the muscle of the muscle-tendon complex.

2 MODELING HUMAN MUSCULOSKELETAL STRUCTURE

2.1 Modeling Muscle Tendon Complex

As introduced in Ref.[8], there are several ways to express muscle tendon complex behaviors. In this study, we deal a three-component model that is composed of contractile element (CE) describing muscle belly, serial elastic element (SE) describing tension of the tendon, and parallel elastic element (PE) describing passive force. Using this model, a muscle force is obtained from the following equation;

$$f_u = a f_{max} f_L f_V cos\alpha, \quad (1)$$

$$= f_{max} f_{SE}, \quad (2)$$

where f_L is tension-length relationship, f_V is force-velocity relationship, f_{SE} is serial elastic force property as respectively shown in Fig.2 (a), (b) and (c). a is the muscle activity level $(0 \leq a \leq 1)$ which represents the input signal from central nervous system. α is the muscle pennation angle.

The tension-length relationship f_L is modeled as follows [9][10]:

$$f_L = e^{-(\bar{l}_m - 1)^2 / S_L}, \quad (3)$$

$$\bar{l}_m = l_m / l_{m0}. \quad (4)$$

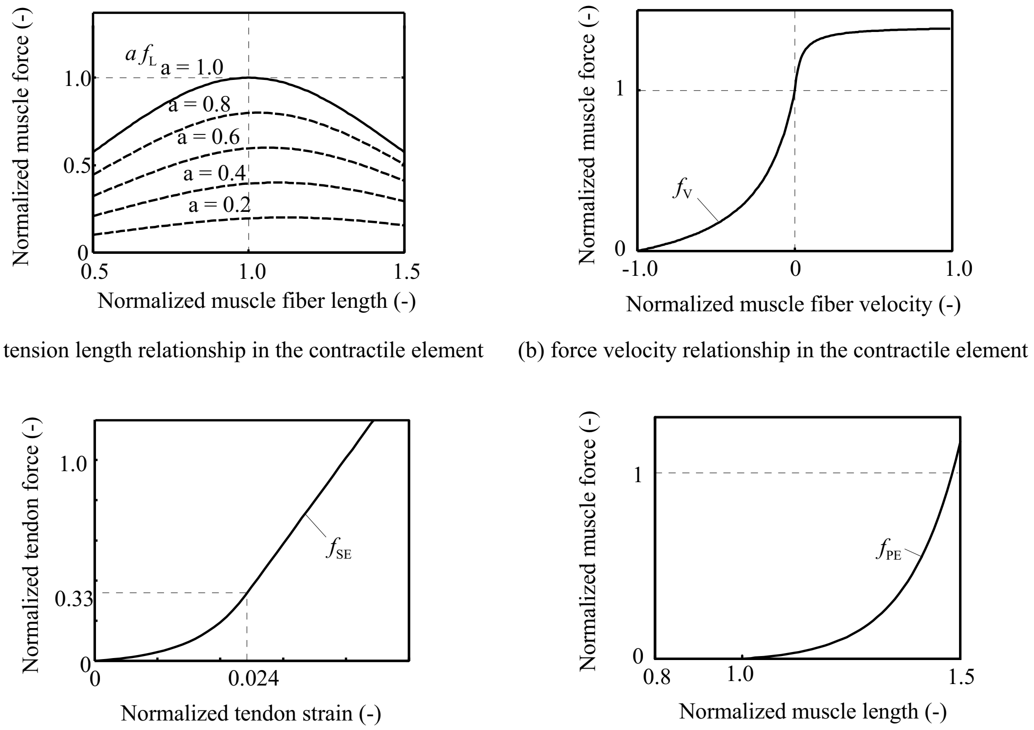

(a) tension length relationship in the contractile element

(b) force velocity relationship in the contractile element

(c) force strain relationship in the series element

(d) tension length relationship in the parallel element

Figure 2: A model of muscle tendon complex and characteristics of the muscle force

$\bar{l}_m$ is the normalized length based on optimal muscle length l_{m0}.

The force-velocity relationship f_V is as follows [9]:

$$
\begin{aligned}
f_V &= \begin{cases} 0 & (\bar{v}_m \leq -1), \\ \frac{1+\bar{v}_m}{1-\bar{v}_m/A_f} & (-1<\bar{v}_m \leq 0), \\ \frac{(B_f-1)+\bar{v}_m(2+2/A_f)B_f}{(B_f-1)+\bar{v}_m(2+2/A_f)} & (\bar{v}_m > 0), \end{cases} && (5) \\
\bar{v}_m &= \dot{l}_m/v_{max}, && (6)
\end{aligned}
$$

where $\bar{v}_m$ is normalized velocity based on maximum contract velocity v_{max}.

The following equations are used to describe the serial elastic element f_{SE} [9],

$$
\begin{aligned}
f_{SE} &= \begin{cases} 0 & (\bar{l}_t \leq 0), \\ \frac{f_{toe}\left(e^{k_{se}\bar{l}_t/\epsilon_{toe}}-1\right)}{e^{k_{se}}-1} & (0<\bar{l}_t \leq \epsilon_{toe}), \\ k_{lin}\left(\bar{l}_t-\epsilon_{toe}\right)+f_{toe} & (\epsilon_{toe}<\bar{l}_t), \end{cases} && (7) \\
\bar{l}_t &= (l_t-l_{t0})/l_{t0}, && (8)
\end{aligned}
$$

where $\bar{l}_t$ is the normalized length based on slack length of the tendon l_{t0}.

As shown in Fig.2 (d), the parallel elastic element f_{PE} is modeled as

$$
\begin{aligned}
f_{PE} &= \frac{e^{k_{pe}(\bar{l}-1)/\epsilon_0}-1}{e^{k_{pe}}-1}, && (9) \\
\bar{l} &= l/(l_{m0}cos\alpha+l_{t0}). && (10)
\end{aligned}
$$

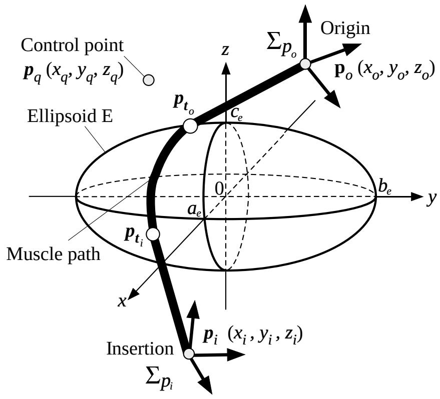

Figure 3: Muscle path wrapping an ellipsoid.

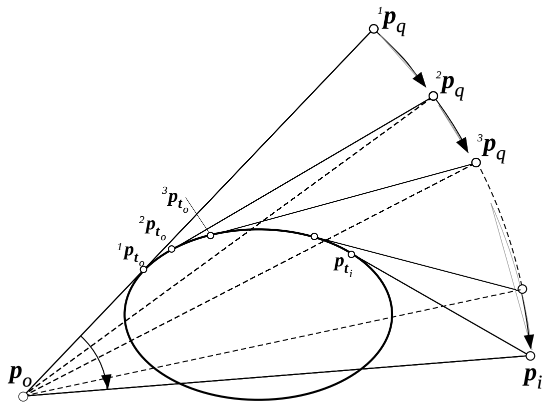

Figure 4: Viapoints along ellipsoid surface.

2.2 Modeling Muscle Path

In modeling a musculoskeletal system of a human body, muscle paths are usually expressed by line segments connecting viapoints between the origin and insertion[2, 3, 4, 5, 6, 7]. However, because the viapoints are fixed to bones that are modeled as rigid bodies, there is a limit to describe smooth muscle paths. Garner et al.[11] and Charlton et al.[12] used a wrapping method to connect between the origin and insertion along with the surface of an ellipsoid, cylinder or cone. These methods, however, need an excessive computational load as convergent calculation is performed on each muscle. In this study, a new wrapping algorithm that allows muscles to conform to an ellipsoid with no convergent calculations are introduced.

As shown in Fig.3, origin and insertion of a muscle are defined as $p_o = (x_o, y_o, z_o)^T$ and $p_i = (x_i, y_i, z_i)^T$ respectively. They are both defined in the frame of a wrapped ellipsoids E, radius of each axis is a_e, b_e, and c_e. Frames Σ_{p_o} and Σ_{p_i} are then defined on these two points. Suppose that Σ_{p_o} move towards the same direction as Σ_{p_i} in the case that Σ_{p_o} is rotated along the axis $u \in \Re^3, |u| = 1$ by ϕ $(0 \leq \phi \leq \pi)$. Then, a control point $p_q = (x_q, y_q, z_q)^T$ is defined as follows

$$p_q = p_o + \eta p_{io} + A(u, \eta\phi)v, \tag{11}$$

where $p_{io} \in \Re^3$ is the vector from point p_o to point p_i, $A(u, \phi) \in \Re^{3\times3}$ is the rotation matrix, $v \in \Re^3$ is an arbitrary constant vector and $0 \leq \eta \leq 1$.

Considering the tangential line of the ellipsoid E that passes through the point p_o and is in the plane containing the points p_o, p_i and p_q. The tangent point $p_{t_o} = (x_t, y_t, z_t)^T$ can be obtained by solving the following system of equations.

$$\frac{{x_t}^2}{{a_e}^2} + \frac{{y_t}^2}{{b_e}^2} + \frac{{z_t}^2}{{c_e}^2} = 1, \tag{12}$$

$$\frac{x_o x_t}{{a_e}^2} + \frac{y_o y_t}{{b_e}^2} + \frac{z_o z_t}{{c_e}^2} = 1, \tag{13}$$

$$\begin{vmatrix} x_t & y_t & z_t & 1 \\ x_o & y_o & z_o & 1 \\ x_q & y_q & z_q & 1 \\ x_i & y_i & z_i & 1 \end{vmatrix} = 0. \tag{14}$$

Although there are two solutions for p_{t_o}, the one with a shorter distance to p_q is selected. Rotating the vector p_{io} in small steps until p_{t_o} coincide p_{t_i}, the above calculation is repeatedly performed with the obtained point being inserted as a viapoint.

Because origin and insertion of muscle are usually on different bones, point p_q moves smoothly depending on movement of the bone. Therefore, if Σ_{p_i}, Σ_{p_o}, η and v are properly defined, it is possible to enhance biofidelity of the muscle path. The algorithm was implemented so as to work well even in the case that multiple ellipsoids are wrapped. Muscles with larger attachment area, such as the broadest muscle of the back and the cowl muscle, are modeled as multiple muscle paths sharing a muscle tendon complex model.

2.3 Formulating Equation of Motion

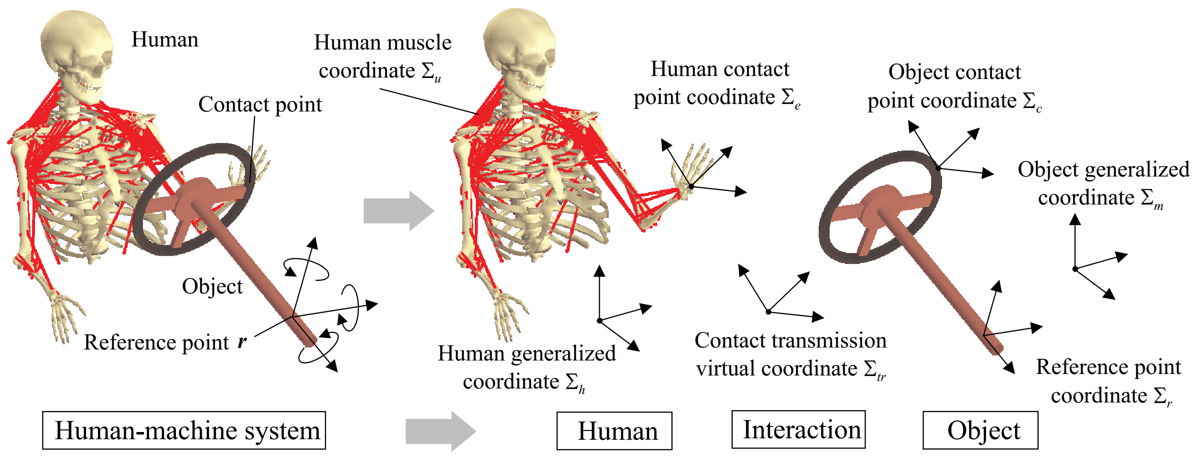

Figure 5: Frames of a human-machine system.

The frames in a human-machine system is illustrated in Fig.5. Σ_u is the frame for the length of the muscle $l_h \in \Re^{n_u}$, n_u is the number of muscles. Σ_h is the frame that is composed of the generalized coordinates $q_h \in \Re^{n_h}$, and that expresses the movement of the human, while Σ_e is the frame for the human's contact with the object and is composed of the contact point coordinate $X_e \in \Re^{c_h}$. Similarly, Σ_m is the frame that expresses the movement of the object and is composed of the generalized coordinates $q_m \in \Re^{n_m}$, while Σ_c is the frame for the object's contact with the human and is composed of the contact point coordinates $X_c \in \Re^{c_m}$. Σ_{tr} is the frame for the n_{tr} dimension that is used to express the transmission of force at the contact point between the human and the object[13, 14]. In the state where the human and the object are in contact, the three frames Σ_e, Σ_{tr} and Σ_c coincide, with their shared z axis oriented in the direction of a line normal to the plane of contact, and assuming that no shifting occurs in the contact point. Σ_r is the frame with its origin at r, the reference point for equivalent impedance characteristics, which can be defined at anywhere on the object.

Each segment of the human body and each part of the object are treated as rigid bodies, where the mass, center of gravity and moment of inertia of each of these rigid bodies are defined. On each body, frames called marker are then defined to describe joints, muscle paths, positions of contact and constraint. In accordance with above definitions and assumptions, an equation of motion for the human-machine system are formulated as the following differential algebraic equations (DAEs),

$$\begin{bmatrix} M & G^T \\ G & 0 \end{bmatrix} \begin{bmatrix} \ddot{q} \\ \lambda \end{bmatrix} = \begin{bmatrix} Q - g - h - J_e^T F_e \\ \gamma \end{bmatrix}, \tag{15}$$

where $M = diag.\left[M_h, M_m\right] \in \Re^{n \times n}, n = n_h + n_m$ is the inertia tensor of the human-machine system consisting of the human inertia $M_h \in \Re^{n_h \times n_h}$ and the object inertia $M_m \in \Re^{n_m \times n_m}$. $q = \left[{q_h}^T, {q_m}^T\right]^T \in \Re^n$ is the vector of the generalized coordinate consisting of $q_h \in \Re^{n_h}$ and $q_m \in \Re^{n_m}$. $G = diag.\left[G_h, G_m\right] \in \Re^{c \times n}$, $c = c_h + c_m$ is the constraint Jacobian. $G_h \in \Re^{c_h \times n_h}, rank(G_h) = c_h < n_h$ is the Jacobian in terms of the human constraint Φ_h. $G_m \in \Re^{c_m \times n_m}, rank(G_m) = c_m < n_m$ is the Jacobian in terms of the object constraint Φ_m and joint constraint of the object Φ_j. $\lambda = \left[F_{\phi_h}^T, \lambda_m^T\right]^T \in \Re^{c_h + c_m}$ is the constraint force and the Lagrange multiplier. In this study, only the holonomic constraint expressed as $G_h \delta q_h = 0$ is considered. $Q = \left[\tau_h^T, Q_m^T\right] \in \Re^n$ is the generalized force. $g = \left[g_h^T, g_m^T\right] \in \Re^n$ is the gravity term. $h = \left[h_h^T, h_m^T\right] \in \Re^n$ is the centrifugal and Coliolis force. $\gamma \in \Re^c$ is the term related to derivative of the constraints. $J_e = \left[J_{e_h}, J_{e_m}\right] \in \Re^{n_c \times n}$ is the Jacobian to contact points between the human and the object. $F_e \in \Re^{n_c}$ is the contact force. In this study, relative coordinates are used to describe the equation of motion of the human body [15], and the absolute coordinates to describe the equation of motion for the object [16]. Therefore, n_h is the total number of the degrees of joint freedom of the human body, and n_m is six times as large as the number of rigid bodies comprising the object model.

3 SOLVING HUMAN-MACHINE SYSTEM

3.1 Solving Inverse Dynamics

Giving motions q, $\dot{q}$, $\ddot{q}$ and forces F_e into the formulated equation of motion Eq.(**??**), generalized force Q is calculated by using a projection method [17] as

$$PM\ddot{q} = P(Q - g - h - J_e^T F_e), \tag{16}$$

where $P \in \Re^{n \times n}$ is the matrix that describes the projection of G onto the null space. In this method, it is unnecessary to calculate the constraint force and the Lagrange multiplier λ. Therefore, the joint torque of the human τ_h can be obtained with the minimum set of input. In this computation, the muscle length vector $L_u \in \Re^{n_u}$ and the muscle contraction velocity $V_u \in \Re^{n_u}$ are also obtained by using muscle paths defined in the human musculoskeletal model. Also, the muscle Jacobian $J_u \in \Re^{n_h \times n_u}$, which indicates the muscle moment arm characteristics, is

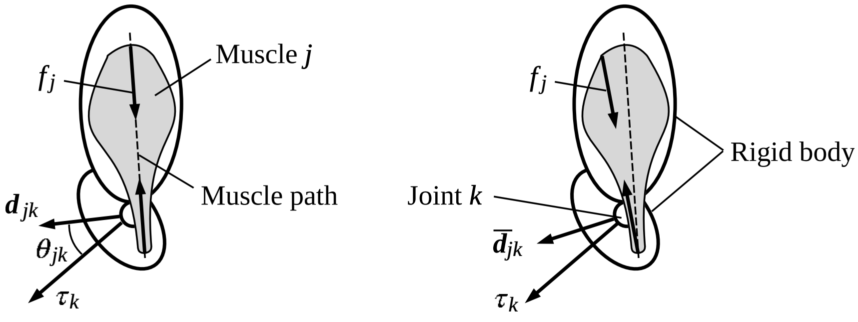

(a) Before conditioning (b) After conditioning

Figure 6: Preconditioning muscle Jacobian

calculated from principle of virtual work.

$$J_u = \frac{\partial L_u}{\partial q_h}. \tag{17}$$

3.2 Preconditioning Muscle Jacobian

Conventional musculoskeletal models assume that the direction of each muscle force is always only on the muscle path line. This assumption might be reasonable if the joint movement is to a limited extent, but in the case of large displacements, it does not hold true because actual muscles have volume and line of action can vary as reported in Ref.[18]. So we process a preconditioning for the muscle Jacobian J_u to give more effectively equilibrium with the human joint torque. Fig.6 illustrates the joint torque τ_k and the moment arm vector d_{jk} before and after the preconditioning. The outline of the algorithm is introduced here, the detail and effectiveness is described in Ref.[19].

Let $\tau_j \in \Re^3$ define the torque vector of j th joint of the human with three rotational degrees of freedom as

$$\tau_j = \left[\tau_i, \tau_{i+1}, \tau_{i+2}\right]^T, \tag{18}$$

where τ_i is i th element of τ_h. Moment arm vector $d_{jk} \in \Re^3$ of muscle k around joint j is also defined as follows,

$$d_{jk} = -\left[J_{k,i}, J_{k,i+1}, J_{k,i+2}\right]^T, \tag{19}$$

where $J_{k,i}$ is (k,i) element of J_u. Then the magnitude of muscle force of muscle k is defined as $f_{u_k} \in \Re^1$, these provide the following equation:

$$\tau_j = \sum_{i=1}^{n_u} d_{jk} f_{u_i}. \tag{20}$$

This indicates that $|d_{jk}|$ represents a magnitude of a joint torque of joint j which is generated by muscle k . The direction of d_{jk} matches that of joint torque of joint j which is generated by muscle k. Therefore, the closer the direction of d_{jk} to that of τ_j, the more efficiently muscle k produce a component of τ_j.

In accordance with the following rules, the moment arm vector d_{jk} are conditioned into $\bar{d}_{jk}$.

$$\bar{d}_{jk} \quad = \quad R_{jk}(\kappa_{jk}, \psi_{jk}) d_{jk}, \tag{21}$$

$$\kappa_{jk} = \frac{d_{jk} \times \tau_j}{|d_{jk}||\tau_j|}, \tag{22}$$

$$\psi_{jk} = \frac{exp(\beta_j - \xi_{jk})}{1 + exp(\beta_j - \xi_{jk})}\xi_{jk}, \tag{23}$$

$$\xi_{jk} = asin\left(\frac{|d_{jk} \times \tau_j|}{|d_{jk}||\tau_j|}\right), \tag{24}$$

where $R_{jk} \in \Re^{3\times3}$ is the rotation matrix, which rotational axis is $\kappa_{jk} \in \Re^3$ and rotation angle is $\psi_{jk} \in \Re^1$. $\xi_{jk} \in \Re^1$ represents the angle between d_{jk} and τ_j. β is the conditioning factor which determines a degree of change in direction of d_{jk}.

Substituting the conditioned moment arm vector $\bar{d}_{jk}$ to corresponding elements of J_u, we can obtain the conditioned muscle Jacobian matrix $\bar{J}_u \in \Re^{n_h \times n_u}$. Consequently, the equilibrium between the joint torques and the muscle forces becomes

$$\tau_h = -\bar{J}_u^T(q_h, \tau_h, \beta) f_u. \tag{25}$$

Note that $\bar{J}_u$ becomes a function of q_h, τ_h and β, so this technique is effective only in inverse dynamics analysis.

3.3 Optimizing Muscle Force Distribution

The muscle force $f_u \in \Re^{n_u}$ can be obtained from the joint torque τ_h according to the following steps. Firstly, the applying joint torque of the human $\tilde{\tau}_h \in \Re^{n_h}$ is calculated eliminating the passive force of the muscle from τ_h,

$$\tilde{\tau}_h = \tau_h + \bar{J}_u^T F_{PE}, \tag{26}$$

where $F_{PE} \in \Re^{n_u}$ is the passive muscle force vector composing of the parallel elastic element of each muscle f_{PE} as describe in Eq.(9).

Therefore, the muscle force f_u can be obtained by solving the constrained optimization problem with

$$minimize \qquad \mathcal{J}(f_u) = f_u^T W^T W f_u, \tag{27}$$

$$subject\ to \qquad \tilde{\tau}_h = -\bar{J}_u^T f_u, \tag{28}$$

$$0 \le f_u \le f_{max}, \tag{29}$$

where $\mathcal{J}(f_u)$ is an objective function of f_u. Eq.(28) is an equality constraint condition of equilibrium between joint torques and muscle forces. Eq.(29) is an inequality constraint condition regarding range of f_u. f_u must be set greater than or equal to 0 because muscle can act only contraction. f_{max} is a maximum muscle force vector. $W \in \Re^{n_u \times n_u}$ is a weighting factor matrix and defined as following equation.

$$W = diag.\{1/k\rho_i g\}, \tag{30}$$

ρ_i is physiological cross sectional area (PCSA) of muscle i and determined refereed to Ref.[20]. k is a coefficient which represents muscle force per unit PCSA and set as 5.5 [21]. g is gravitational acceleration. An et al [22] showed that the muscle force obtained from the objective function using Eq.(30) is consistent with the muscle activity distribution obtained by measuring electromyography (EMG). In this study, the above equation is solved by using sequential quadratic programming [23].

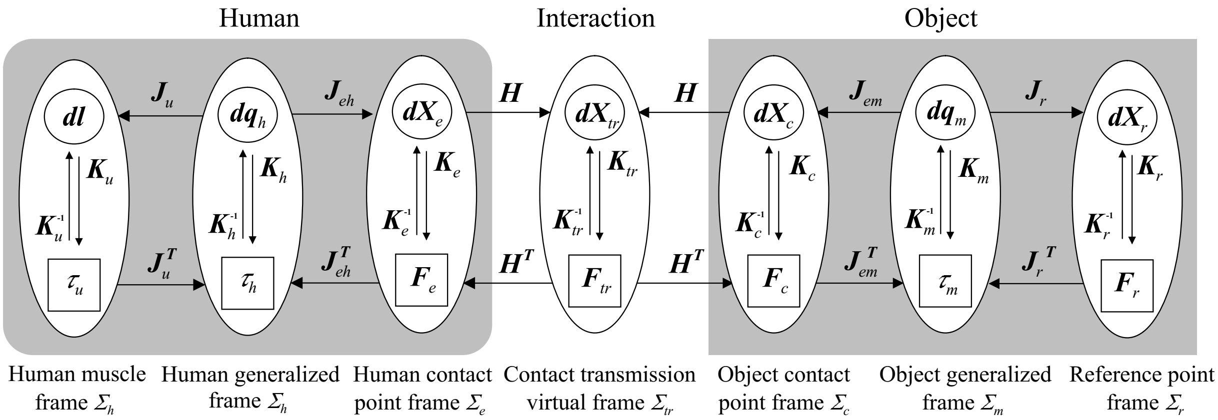

Figure 7: Force/displacement relationships of a human-machine system.

4 ANALYZING EQUIVALENT IMPEDANCE CHARACTERISTICS

In this section, we describe a method for obtaining the muscle stiffness $K_u \in \Re^{n_u \times n_u}$ and muscle viscosity $B_u \in \Re^{n_u \times n_u}$ from the muscle force f_u. Then the human muscle impedance is transformed into reference points r, according to both coordinate transformation of tensor and an orthogonal complementary projection technique [17].

4.1 Muscle Stiffness and Viscosity

By using Eq.(1), activity level of the muscle $a \in \Re^{n_u}$ is calculated as

$$a = \frac{f_u}{f_{max} f_L f_V cos\alpha}. \tag{31}$$

The muscle stiffness k_m and tendon stiffness k_t are calculated by partial differentiation of Eq.(1) and (2) with respect to the muscle length as follows;

$$k_m = a f_{max} \frac{\partial f_L}{\partial l_m} f_V cos\alpha, \tag{32}$$

$$k_t = f_{max} \frac{\partial f_{SE}}{\partial l_t}. \tag{33}$$

Further, the muscle-tendon complex stiffness k_{u_i} is expressed by:

$$k_u = \frac{k_m k_t}{k_m + k_t}, \tag{34}$$

and the stiffness of the parallel elastic element k_p is expressed by:

$$k_p = f_{max} \frac{\partial f_{PE}}{\partial l_u} cos\alpha. \tag{35}$$

Making up $k_u \in \Re^{n_u}$, $k_t \in \Re^{n_u}$ and $k_p \in \Re^{n_u}$ from k_u, k_t and k_p of each muscle, The muscle stiffness matrices becomes

$$K_u = diag.\{k_u\}, \tag{36}$$

$$K_{ut} = diag.\{k_t\}, \tag{37}$$

$$K_{up} = diag.\{k_p\}. \tag{38}$$

$K_u \in \Re^{n_u \times n_u}$ expresses the stiffness of the muscle-tendon complex, $K_{ut} \in \Re^{n_u \times n_u}$ is the stiffness of the tendon, and $K_{up} \in \Re^{n_u \times n_u}$ is the passive stiffness of the parallel elastic element. In the same manner as described above, the muscle viscosity matrices are obtained by partially differentiating Eq.(1) with respect to the muscle velocity.

4.2 Stiffness Transformation

Fig.7 illustrates relationships between force and displacement of a human-machine system. According to tensor coordinate transformation, the muscle stiffness K_u and K_{up} in the muscle frame Σ_u are transformed into the human stiffness $K_h \in \Re^{n_h \times n_h}$ expressed in Σ_h

$$K_h = J_u^T K_u J_u + J_u^T K_{up} J_u. \tag{39}$$

Here, by using $P_h \in \Re^{n_h \times n_h}$, orthogonal complementary projection of G_h, $P_h G_h^T = 0$, the constrained stiffness $K'_h \in \Re^{n_h \times n_h}$ and the constrained Jacobian $\bar{J}_e \in \Re^{n_e \times n_h}$ can be obtained as follows:

$$\begin{aligned} K'_h &= K_h + P_h K_h - (P_h K_h)^T, & (40) \\ \bar{J}_{e_h} &= J_{e_h} P_h. & (41) \end{aligned}$$

Furthermore, considering contact constraint matrix H [13, 14] and the internal force effect of the contact force F_c, the constrained equivalent stiffness of the human in Σ_m, ${}^hK'_m \in \Re^{n_m \times n_m}$, becomes

$$\begin{aligned} {}^hK'_m &= {}^hK'_{mj} + {}^hK'_{mf}, & (42) \\ {}^hK'_{mj} &= J_{e_m}^T H^T (H\ K_e'^{-1} H^T)^{-1} H J_{e_m}, & (43) \\ K'_e &= (\bar{J}_{e_h} K_h'^{-1} \bar{J}_{e_h}^T)^{-1}, & (44) \\ {}^hK'_{mf} &= \frac{\partial J_{e_m}^T F_c}{\partial q_m}, & (45) \end{aligned}$$

where ${}^hK'_{mj} \in \Re^{n_m \times n_m}$ is the equivalent stiffness transmitted from the muscle stiffness K_u, and ${}^hK'_{mf} \in \Re^{n_m \times n_m}$ the stiffness due to the internal force effect by F_c.

Now, by adding the object stiffness $K_m \in \Re^{n_m \times n_m}$ in Σ_m, and considering the constraint on the object Φ_m in the same manner as be done with Eq. (40) and (41), we have

$$\begin{aligned} {}^{hm}K''_m &= {}^{hm}K'_m + P_m {}^{hm}K'_m - (P_m {}^{hm}K'_m)^T, & (46) \\ {}^{hm}K'_m &= {}^hK'_m + K_m, & (47) \\ \bar{J}_r &= J_r P_m, & (48) \end{aligned}$$

where $P_m \in \Re^{n_m \times n_m}$ is the orthogonal complementary projection of G_m, $P_m G_m{}^T = 0$, $\bar{J}_r \in \Re^{n_r \times n_m}$ is the constrained Jacobian matrix on the reference r of the object.

Therefore, the equivalent stiffness of the human-machine system ${}^{hm}K''_m \in \Re^{n_r \times n_r}$ taking the constraints on both the human and the object into consideration can be expressed by

$${}^{hm}K''_r = (\bar{J}_r {}^{hm}K_m''^{-1} \bar{J}_r^T)^{-1}. \tag{49}$$

Meanwhile the equivalent viscosity ${}^{hm}B''_m \in \Re^{n_r \times n_r}$ can be obtained by defining the muscle viscosity $B_u \in \Re^{n_u \times n_u}$ instead of the muscle stiffness K_u, and performing similar transformation without the second term of Eq.(42).

Proof of Eq. (40)

If the generalized force Q can be expressed by stiffness $K \in \Re^{n\times n}$ and infinitesimal displacement $\delta q \in \Re^n$ as follows:

$$Q = K\delta q, \tag{50}$$

The equation of motion for a multibody system that is constrained by the environment is described as

$$M\ddot{q} + g + h + G^T\lambda = K\delta q. \tag{51}$$

Considering the static condition, $\ddot{q} = \dot{q} = 0$. Then Eq.(51) becomes

$$g + G^T\lambda = K\delta q. \tag{52}$$

While the constraint can be expressed by the Jacobian matrix G and the infinitesimal displacement δq as follows:

$$G\delta q = -c, \tag{53}$$

where $c = \partial\Phi/\partial t \in \Re^{c_h+c_m}$. Multiplying both sides of Eq.(52) by the matrix P,

$$Pg = PK\delta q \tag{54}$$

is obtained. Eq.(53) can be expressed using the pseudo inverse matrix of G, G^+ [17];

$$(I - P)\delta q = -G^+c. \tag{55}$$

Premultiplying both sides of Eq. (55) by K, adding Eq.(54) to the result, and rearranging the equation and taking into consideration $P^T = P$, $K^T = K$,

$$Pg - KG^+c = \left\{K + PK - (PK)^T\right\}\delta q \tag{56}$$

is obtained.

The second term on the left hand side of Eq.(56) becomes 0 if the displacement constraint is not included; therefore, Eq.(56) can be expressed by

$$Pg = \left\{K + PK - (PK)^T\right\}\delta q. \tag{57}$$

Comparing Eq.(57) with Eq.(50), the right hand side of Eq.(57) satisfies the constraint and is equal to elastic force due to the infinitesimal displacements δq. Therefore, $K + PK - (PK)^T$ can be regard as the stiffness taking the constraint Φ into consideration.

4.3 Inertia Transformation [24]

Fig.8 illustrates relationships between force and acceleration in a human-machine system. In the same manner as in the stiffness transformation, the constrained inertia matrix $M'_h \in \Re^{n_h\times n_h}$ is

$$M'_h = M_h + P_hM_h - (P_hM_h)^T. \tag{58}$$

The detail of derivation is in Ref.[17]. Then the equivalent inertia ${}^hM'_m \in \Re^{n_m\times n_m}$ in Σ_m can be obtained as

$$\begin{aligned} {}^hM'_m &= J^T_{e_m}H^T(H\,{}^hM'^{-1}_e H^T)^{-1}HJ_{e_m}, & (59)\\ {}^hM'_e &= (\bar{J}_{e_h}M'^{-1}_h\bar{J}^T_{e_h})^{-1}. & (60) \end{aligned}$$

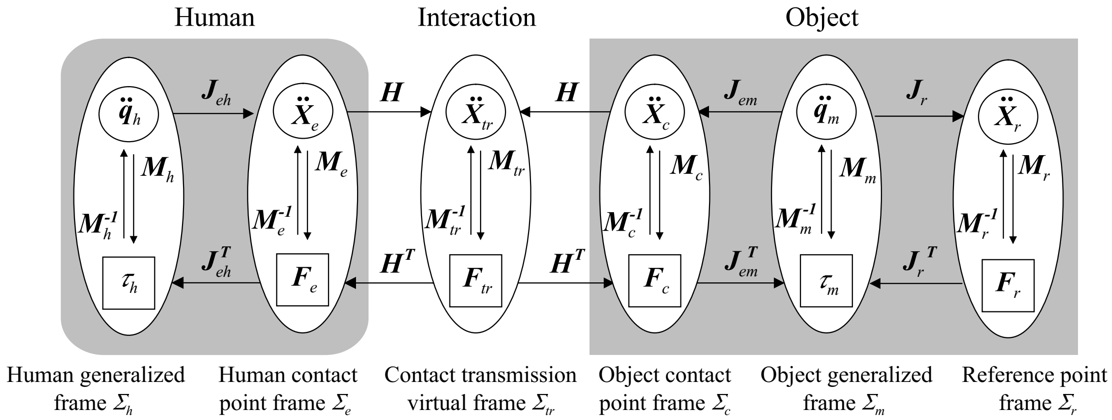

Figure 8: Force/acceleration relationships of a human-machine system.

By using orthogonal complementary projection of G_m, we have

$$
\begin{aligned}
{}^{hm}M''_m &= {}^{hm}M'_m + {}^{hm}\overline{M}'_m, && (61)\\
{}^{hm}\overline{M}'_m &= P_m {}^{hm}M'_m - (P_m {}^{hm}M'_m)^T, && (62)\\
{}^{hm}M'_m &= {}^{h}M'_m + M_m. && (63)
\end{aligned}
$$

Therefore, the equivalent inertia of the human-machine system ${}^{hm}M''_r \in \Re^{n_r \times n_r}$ taking the constraints on both the human and the object into consideration can be expressed by

$$
{}^{hm}M''_r = (\bar{J}_r {}^{hm}M''^{-1}_m \bar{J}_r^{\,T})^{-1}. \tag{64}
$$

The above gives the detailed method for calculating the equivalent impedance characteristics of a human-machine system under constrained environment. In the next section, using this method, we configure a three dimensional model for a driver-steering system and analyze the equivalent impedance characteristics for a steering maneuver.

5 APPLICATION TO UPPER EXTREMITIES MOTION

In order to demonstrate the effectiveness of the proposed analysis described above, a forklift truck steering operation were measured measured and analyzed using a musculoskeletal model of upper extremities. The subject was a male, skilled in operating industrial vehicles, 36 years old, 1.83 m tall, and weighing 80.0 kg.

5.1 Experimental Setups

Fig. 9 depicts the experimental setup consisting of an driving position adjustable mockup, a steering column with a DC motor, a steering control computer, a steering unit for measuring operation force of the subject, a liquid crystal display monitor, an electromyographies monitor, and a motion capture system. Longitudinal and vertical position of the steering column and the seat, inclination angle of the steering unit can be changed to correspond to various type of vehicles. In this study, the layout parameters listed in the Fig.9 were set.

As shown in Fig.10, a round bar with a counter weight was attached to the head of the column; the operation force that the subject exerts on it was measured by a force/torque transducer(ATI NANO25, load rating:125N/3Nm). A bearing was fitted between the knob and the

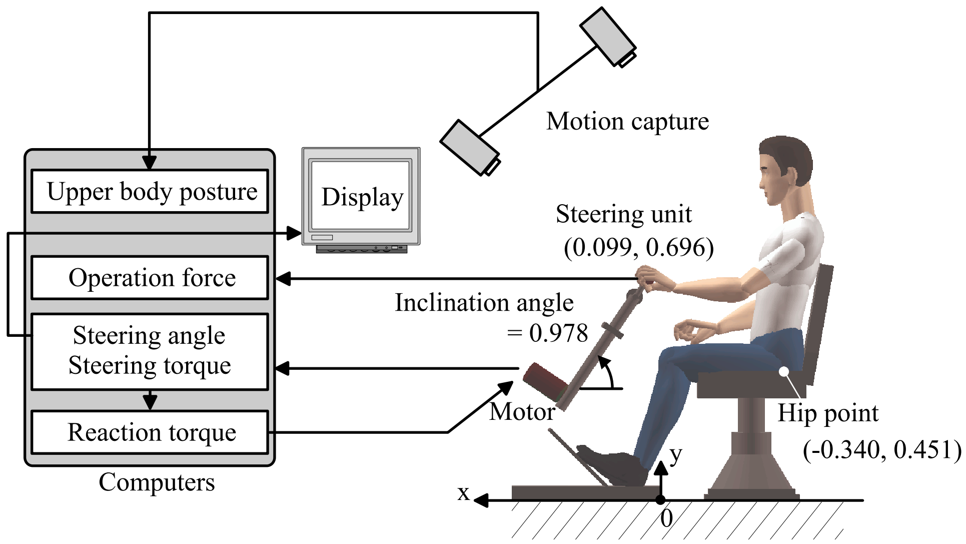

Figure 9: Experimental setups.

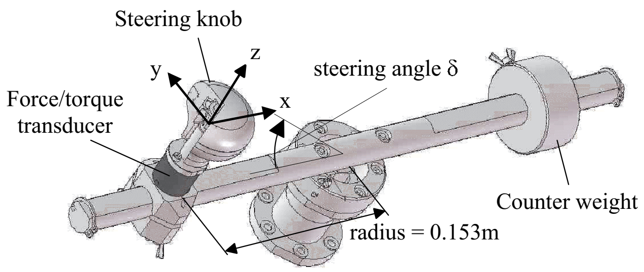

Figure 10: Steering unit.

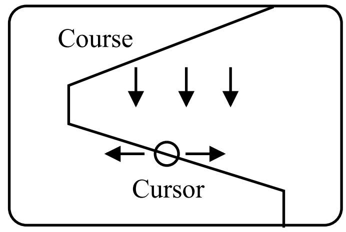

Figure 11: Example of display.

supporting part, so that the torque around the z axis in Fig.10 was not transmitted. Hence H in Eq. (43) and (59) can be expressed by:

$$H = \begin{bmatrix} 1 & 0 & 0 & 0 & 0 & 0 \\ 0 & 1 & 0 & 0 & 0 & 0 \\ 0 & 0 & 1 & 0 & 0 & 0 \\ 0 & 0 & 0 & 1 & 0 & 0 \\ 0 & 0 & 0 & 0 & 1 & 0 \end{bmatrix}. \tag{65}$$

As a subject operate the steering unit, the reaction torque was given to the subject generated in DC motor (rated load torque: 2.25Nm, gear ratio: 14.67). A rotary encoder (Danaher, 5000pulse/rotation) was attached to the motor, and a torque sensor (Kistler***) was placed at the head of the column. In the steering control unit, the reaction torque was kept at the value of 1.2 Nm by using angular velocity and torque feedback.

Fig.11 shows an illustration of the task. A target course was continually shown from the upper part of the display. The cursor in the display was moved from side to side depending on the angle of the steering unit.

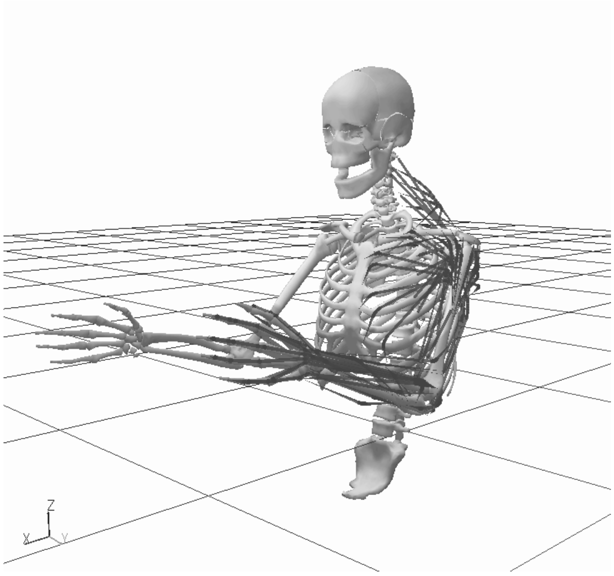

Figure 12: A musculoskeletal model of upper extremities.

S_L	v_{max}	A_f	B_f	f_{toe}	ϵ_{toe}	k_{se}	k_{lin}	k_{pe}	ϵ_0
0.45	10 l_{m0}	0.25	1.4	0.33	0.0241	3.0	42.8	5.00	0.60

Table 1: Physiological parameters for the muscle model [9].

5.2 Musculoskeletal Model of Upper Extremities

A musculoskeletal model of the upper extremities was scaled to the subject as shown in Fig.12. The model consists of 29 muscles and 9 rigid bodies including the upper arms, fore arms and hands. The origins and insertions, optimal length, maximum force of the muscles were refereed to such as Ref.[20] and so on. The muscle moment arm characteristics were also adjusted according to published literature such as [25] and so on. Furthermore, the mass and moment of inertia of each rigid body were set after referring to Ref.[26]. The physiological parameters for each muscle are shown in Table 1. The pennation angle α is treated as 0, precondition factor β as $\pi/18$ for all muscles.

5.3 Experimental Method

The subject sat on the driving position-adjustable bench, and gripped the steering knob with his left hand. The subject was instructed to follow the course by turning the steering wheel counterclockwise six times at a speed of 2π rad/sec, stopping it at the 9 o'clock position, holding it there for about one second, turning it clockwise six times, and then stopping it again at the 9 o'clock position. The posture of the upper body while operating was measured using motion capture (Motionanalysis EAGLE). In this study, 30 markers was attached and the three dimensional positions of them were measured using 10 cameras. the operating force of the hand was measured using the force/torque transducer, and measured values were used as inputs for the following analysis. Electromyograph of four different muscles around the joint of the left shoulder were also measured for verification.

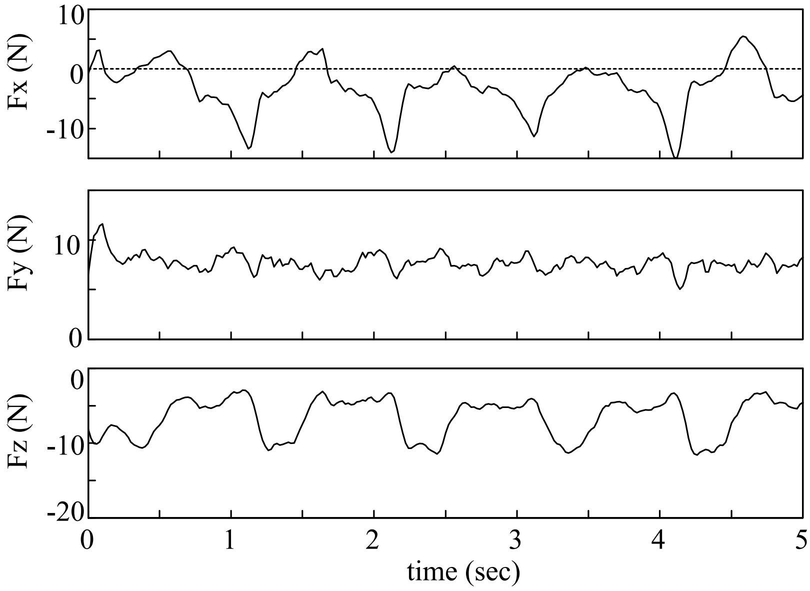

Figure 13: Measured operation force during clockwise rotation.

5.4 Equivalent impedance of the Hand

Fig.13 shows the measured operation force for clockwise rotation. The tangential force, F_y, required to rotate the steering wheel was held constant at around 8.0N. On the other hand, the patterns of the normal force F_x and the pressing force F_z vary depending on the position of the knob. The operation force for clockwise rotation and the operational posture data were analyzed using the musculoskeletal model.

Fig.14 shows the estimated muscle force of the anterior and posterior of the deltoideus over four times of clockwise turning. Rectified and filtered EMG data are also shown in the Fig.14. The horizontal axis is normalized based on the knob position such that the 9 o'clock position is 0. Fig.15 (a) shows the equivalent inertia ellipsoids of the hand at four different positions. Contraction patterns of both muscles are in good agreement with measurement results. The size, shape and direction of the inertia ellipsoid closely approximate the results of hand impedance estimated when the posture is maintained [27]. Considering these two results, it is thought that both the estimated muscle force and the equivalent impedance calculated by this analysis are appropriate.

On the other hand, Fig.15 (b) shows a stiffness ellipsoid drawn by hand stiffness ${}^{h}K'_{mj}$ based on the stiffness K_u of muscles in motion. The size of the ellipsoid is considerably smaller than that estimated by Tsuji et al.[27]. This is thought to be attributed to the equivalent stiffness identified by Tsuji et al. containing the effects of reflection, whereas, in this method, the equivalent stiffness was calculated without taking into account the effects of reflection, skin, tissues, etc.

5.5 Equivalent Impedance around the Steering Column

The equivalent inertia ${}^{hm}M''_r \in \Re^1$ and the equivalent stiffness ${}^{hm}K''_r \in \Re^1$ around the steering column axis was calculated. Thinking of the previous result on the equivalent stiffness, ${}^{hm}K''_r$ was also decomposed of the equivalent stiffness due to the muscle ${}^{hm}K''_{rj} \in \Re^1$ the equivalent stiffness due to the internal force effect ${}^{hm}K''_{rf} \in \Re^1$. In the calculation, the inertia and

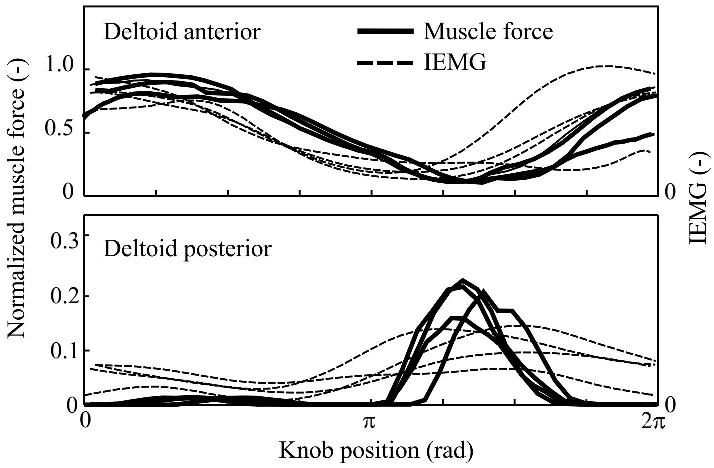

Figure 14: Comparison of muscle force with IDEM during clockwise rotation.

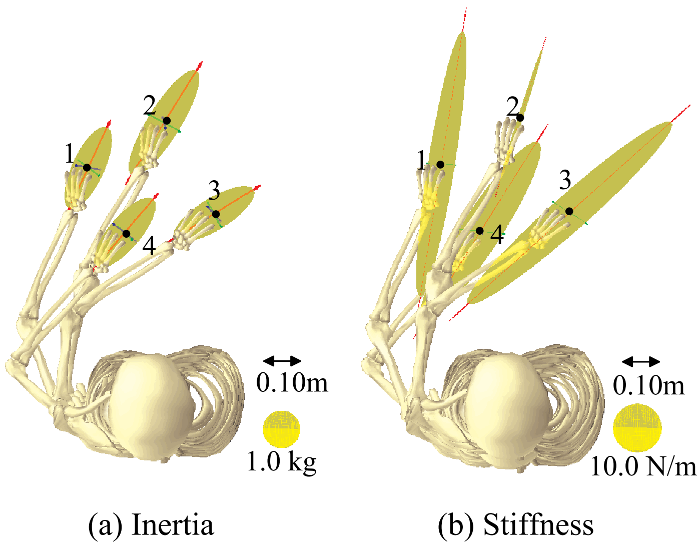

Figure 15: Simulated stiffness and inertia ellipsoids at different postures during clockwise rotation.

stiffness of the steering unit was assumed to be 0, being necessary to clarify the effects of the human. The results are plotted in Fig.16, lateral axis is normalized same as in Fig.14.

As for the equivalent inertia ${}^{hm}M''_r$, there is a region where it contributes greatly to the steering column axis, while there is another region where it hardly contributes at all. Comparing with Fig.15(a), it is found that the equivalent inertia ${}^{hm}M''_r$ increases in a region where a longer axis of the hand inertia ellipsoid approaches the tangential direction of the steering, while it decreases in a region where a shorter axis of the hand inertia ellipsoid approaches the tangential direction of the steering.

It should be noted that as the equivalent stiffness ${}^{hm}K''_r$ is affected by internal force, it takes on a negative value when the knob is at a position where the hand is almost fully extended. This is because the subject turns the steering wheel at an angular speed of 2 rad/sec, causing the operator to exert an operation force inwards in the direction of a normal line. According to the results of a crank turning experiment conducted by Ota, et al.[28], it is pointed out that the hand force works inwards in the direction of a normal line. Equivalent stiffness may attain a positive value in the actual steering operation. However, the steering operation of this human-machine

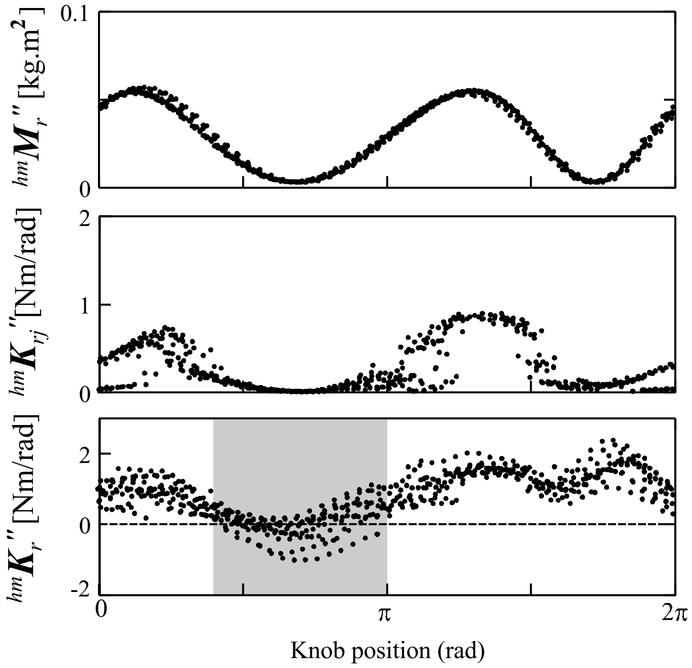

Figure 16: Equivalent inertia and stiffness around steering column axis during clockwise rotation.

system may be made more stable if the effects of internal force and those of muscle stiffness are properly combined. Also, if a method of allowing equivalent stiffness to become positive in all regions can be developed by controlling the operation system configuration.

6 CONCLUSIONS

In this paper, we propose a method for analyzing equivalent impedance characteristics of human-machine systems considering not only contact between the human and the object but also constraint on the human and on the object. The proposed analysis was applied to the upper extremities motion in forklift steering operation. The results reveal that this analysis is an useful tool in examining the physical significance of human-machine systems and can be effective in designing a human-machine system.

The proposed method can easily apply to other type of motions, and objective functions in the muscle force estimation. However, we think that the musculoskeletal model will need further improvements in accuracy. More physiological experimental data and moment arm characteristics in complex joint movements will be required in order to define accurate parameters of the muscle model and muscle path. More studies are needed concerning validation of the impedance characteristics during steering and other behaviors. Furthermore, a new solution would be necessary if one taking effects of muscle activation dynamics and reflective feedback into consideration.

REFERENCES

[1] F.E.Zajac: Muscle and Tendon: Properties, Models, Scaling, and Application to Biomechanics and Motor Control, *Critical Reviews in Biomedical Engineering*, **17-4**, 359–411, 1989.

[2] S.L.Delp, J.P.Loan: A Graphics-based Software system to develop and analyze models of musculoskeletal structures, *Comput, Biol. Med.*,**25**, 21–34, 1995.

[3] P.Eberhard et al.: Investigations for the Dynamical Analysis of Human Motion, *Multibody System Dynamics*, **3**, 1–20, 1999.

[4] J.Rasmussen et al.: AnyBody - a software system for ergonomic optimization, Proceedings of the 5th World Congress on Structural and Multidisciplinary Optimization, 2003.

[5] Y.Nakamura, et al.: Somatosensory Computation for Man-Machine Interface From Motion-Capture Data and Musculoskeletal Human Model, *IEEE Trans. on Robotics*, **21**-1 58–66, 2005.

[6] Y. Takeda, et al.: Impedance Simulator : Analysis of Human Hand Impedance Characteristics, Proceedings of the 2nd International Symposium on Measurement, Analysis and Modeling of Human Functions, 2004.

[7] S. Stroeve: Neuromuscular control model of the arm including feedback and feedforward components, *Acta Psychologica*, **100**, 117–131, 1998.

[8] J.M. Winters: Hill-Based Muscle Models: A Systems Engineering Perspective, *Multiple Muscle Systems: Biomechanics and Movement Organizations*, Springer-Verlag, 69–93, 1990.

[9] D.G. Thelen: Adjustment of Muscle Mechanics Model Parameters to Simulate Dynamic Contractions in Older Adults, *Transactions of the ASME*, **1**25, 70–77, 2003.

[10] D.G. Lloyd and T.F. Besier: An EMG-driven musculoskeletal model to estimate muscle forces and knee joint moments in vivo, *Journal of Biomechanics*,**3**6, 765–776, 2003.

[11] B.A.Garner, M.G.Pandy: The obstacle-set method for representing muscle paths in musculoskeletal models, *Computer methods in biomechanics and biomedical engineering*, **3**, 1–30, 2000.

[12] I.W.Charlton, G.R.Johnson: Application of spherical and cylindrical wrapping algorithms in a musculoskeletal model of the upper limb, *Journal of Biomechanics*, **34-9**, 1209–1216, 2001.

[13] M.R. Cutkosky and I. Kao: Computing and Controlling the Compliance of a Robotic Hand, *IEEE Transaction on Robotics and Automation*,**5-2**, 151–165, 1989.

[14] A. Jazidie, T. Tsuji, M. Nagamachi and K. Ito: Multi-Point Compliance Control for Dual-Arm Robots Utilizing Kinematics Redundancy, *Trans. of the SICE*,**2**9-6, 637–646, 1993.

[15] R.P.Paul *Robot Manipulators: Mathematics, programming, and control*, The MIT Press, 1981.

[16] P.E. Nikravesh *Computer-Aided Analysis of Mechanical Systems*. Prentice-Hall, Englewood Cliffs, New Jersey, 1988.

[17] F. Aghili, J. C. Piedbcæuf: Simulation of Motion of Constrained Multibody Systems Based on Projection Operator, *Multibody System Dynamics*, **10-1**, 3–16, 2003.

[18] G. P. Pappas, D.S.Asakawa, S.L.Delp, F.E.Zajac, J.E.Drace : Nonuniform shortening in the biceps brachii during elbow flexion, *Journal of Applied Physiology*, **92**, 2381–2389, 2002.

[19] D.Yamada, M.Hada: An Estimation Method of Muscle Force by Variable Moment Arm Vector, Proceeding of the 10th Digital Human Modeling for Design and Engineering Conference, **2007-01-2468**, 2007.

[20] G.T. Yamaguchi, A.G.U. Sawa, D.W. Moran, M.J. Fessler and J.M. Winters: A Survey of Human Musculotendon Actuator Parameters, *Multiple Muscle Systems: Biomechanics and Movement Organizations*, Springer-Verlag, 717–773, 1990.

[21] C. Gans: Fiber architecture and muscle function. *Exercise and Sports Sciences Reviews*, **10**, 106–107, 1982.

[22] K.N. An, B.M. Kwak, E.Y. Chao and B.F. Morrey: Determination of muscle and joint forces: A new technique to solve the indeterminate problem, *Trans. of the ASME*,**1**06-4, 364–367, 1984.

[23] P.E. Gill, W. Murray and M.A. Saunders: SNOPT: An SQP Algorithm for Large-Scale Constrained Optimization, *SIAM Review*, **4**7-1, 99–131, 2005.

[24] M.Hada et al.: Equivalent Inertia of Human-Machine Systems under Constraint Environments, Proceeding of the 3rd Asian Conference on Multibody Dynamics, Tokyo,Japan, A00643, 2006.

[25] W.M.Murray, S.L.Delp, T.S.Buchanan：Variation of muscle moment arms with elbow and forearm position *Journal of Biomechanics*, **28-5**, 513–525, 1995.

[26] R.F. Chandler: *Investigation of inertia properties of the human body*, AMRL-TR-74-137, 1975.

[27] T. Tsuji, et al.: Human hand impedance characteristics during maintained posture, *Biological Cybernetics*, **72**, 475–485, 1995.

[28] K.Ohta, M.M.Svinin, Z.Luo, S.Hosoe, and R.Laboissiere: Optimal trajectory formation of constrained human arm reaching movements, *Biological Cybernetics*, **91-1**, 23–36, 2004.